PHYSICAL REVIEW D **76,** 074028 (2007)

Investigation of a_0–f_0 mixing

Christoph Hanhart,[1,*] Bastian Kubis,[2,†] and José R. Peláez[3,‡]

[1]*Institut für Kernphysik (Theorie), Forschungzentrum Jülich, D-52425 Jülich, Germany*
[2]*HISKP (Theorie), Universität Bonn, Nussallee 14-16, D-53115 Bonn, Germany*
[3]*Departamento de Física Teórica II, Universidad Complutense, E-28040, Madrid, Spain*

(Received 3 July 2007; published 19 October 2007)

We investigate the isospin-violating mixing of the light scalar mesons $a_0(980)$ and $f_0(980)$ within the unitarized chiral approach. Isospin-violating effects are considered to leading order in the quark mass differences and electromagnetism. In this approach both mesons are generated through meson-meson dynamics. Our results provide a description of the mixing phenomenon within a framework consistent with chiral symmetry and unitarity, where these resonances are not predominantly $q\bar{q}$ states. Amongst the possible experimental signals, we discuss observable consequences for the reaction $J/\Psi \to \phi\pi^0\eta$ in detail. In particular, we demonstrate that the effect of a_0–f_0 mixing is by far the most important isospin-breaking effect in the resonance region and can indeed be extracted from experiment.

DOI: 10.1103/PhysRevD.76.074028 PACS numbers: 13.20.Gd, 12.39.Fe, 13.40.Ks

I. INTRODUCTION

Although the light scalar mesons $a_0(980)$ and $f_0(980)$ have been established as resonances long ago, there is still a heated debate going on in the literature regarding the very nature of these states. Naively, one might assign them a conventional $q\bar{q}$ structure, however, at present no quark model is capable of describing both states simultaneously as $q\bar{q}$ states—see, e.g., Ref. [1]. On the other hand, as early as 1977 it was stressed that especially in the scalar channel the interaction of four-quark systems (two quarks, two antiquarks) is attractive [2]. Some authors have found indications for the existence of compact four-quark states [3,4]. However, the same short-ranged interaction can also be the kernel to the scattering of pseudoscalars, giving rise to extended four-quark states that one might call hadronic molecules or extraordinary hadrons [5–8]. Independently, a similar conclusion was found in different approaches [9–14].

A very different approach to quantify the nature of scalar states was presented in Ref. [15], where it was argued that the value of the effective coupling constant of a resonance to a particular continuum channel is a direct measure of its molecular component if the corresponding threshold is very close to the resonance position. When applied to the case of the $f_0(980)$ also this model-independent analysis revealed that this scalar is (to a very large degree) of molecular nature [15]. This picture was further supported by analyses of the reactions $\phi \to \pi^0\pi^0\gamma$ and $f_0 \to \gamma\gamma$ [16,17]. For the $a_0(980)$, on the other hand, no clear picture emerged from these studies (note that also the data is of poorer quality). This might either mean that the physical $a_0(980)$ has some sizable admixture of something different from $K\bar{K}$ or is a virtual state. Here more information is urgently called for.

An observable supposedly of high sensitivity to the structure of the scalar mesons was identified at the end of the 1970s, when Achasov and co-workers observed that the isospin-violating mixing of the isovector a_0 and the isoscalar f_0 should be significantly enhanced due to the proximity of the kaon thresholds to the poles of both mesons. In Ref. [18] it was demonstrated that the leading piece of the a_0–f_0 mixing amplitude can be written as

$$\begin{aligned}\Lambda_L &= \langle f_0|T|a_0\rangle \\ &= ig_{f_0K\bar{K}}g_{a_0K\bar{K}}\sqrt{s}(p_{K^0} - p_{K^+}) + \mathcal{O}(p_{K^0}^2 - p_{K^+}^2),\end{aligned} \tag{1}$$

where $p_{K^{0,+}}$ denotes the modulus of the relative momenta of the neutral and charged-kaon pairs, respectively, and the effective coupling constants are defined through $\Gamma_{RK\bar{K}} = g_{RK\bar{K}}^2 p_K$, $R = a_0, f_0$. Obviously, this leading contribution is just the difference of the unitarity cut contributions of the diagrams shown in Fig. 1 and is therefore model independent. In addition, the signal is proportional to the effective coupling constants of the scalar mesons that encode the essential structure information, as outlined above. As already stressed in Ref. [18], the contribution shown in Eq. (1) is unusually enhanced between the K^+K^- and the $K^0\bar{K}^0$ thresholds, a regime of only 8 MeV width. Here it scales as

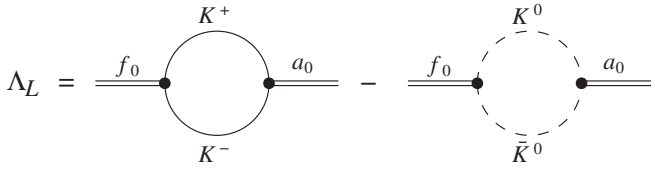

FIG. 1. Graphical illustration of the leading contribution to the a_0–f_0 mixing matrix element Λ_L defined in Eq. (1).

*c.hanhart@fz-juelich.de
†kubis@itkp.uni-bonn.de
‡jrpelaez@fis.ucm.es

$$\sqrt{\frac{M_{K^0}^2 - M_{K^+}^2}{M_{K^0}^2 + M_{K^+}^2}} \sim \sqrt{\frac{m_d - m_u}{m_s + \hat{m}}}, \quad (2)$$

where m_u, m_d, and m_s denote the current quark masses of the up, down, and strange quark, respectively, $\hat{m} = (m_u + m_d)/2$, and we neglect electromagnetic effects in the kaon masses for this rather symbolic formula. This is in contrast to common isospin-violating effects[1] which scale as $(m_d - m_u)/m_s$, since they have to be analytic in the quark masses. It is easy to see that away from the kaon thresholds Λ returns to a value of natural size. In the phenomenological calculation of Ref. [19] this effect was confirmed, however, also there the different kaon masses were the only source of isospin violation.

A subleading contribution to the mixing amplitude is given, in the resonance picture, by isospin-violating couplings of the resonances to the two-kaon continuum $g^I_{RK\bar{K}}$ as depicted in Fig. 2,

$$\Lambda_V = i(g^I_{f_0 K\bar{K}} g_{a_0 K\bar{K}} + g_{f_0 K\bar{K}} g^I_{a_0 K\bar{K}})\sqrt{s} p_K + \mathcal{O}(p_K^2). \quad (3)$$

Although these effects are regular in the isospin-breaking parameter, i.e. of order $m_d - m_u$, they are kinematically enhanced due to the unitarity cut $\propto p_K$. An assessment of the size of such effects obviously relies on an estimate of the isospin-violating couplings $g^I_{RK\bar{K}}$ that we will provide in this paper. It should be stressed, however, that as their isospin-conserving counterparts, the $g^I_{RK\bar{K}}$ are well defined, observable quantities.

In addition, there can also be mixing through the exchange of soft photons in meson loops—see Fig. 3—giving rise to the mixing amplitude Λ_P. The full mixing amplitude is then given by

$$\Lambda = \Lambda_L + \Lambda_V + \Lambda_P. \quad (4)$$

If a_0 and f_0 had a significant admixture from elementary scalars, one should in addition expect a direct a_0–f_0 transition to appear. However, this is not included in our approach.

Our purpose is to improve on the theoretical understanding of the possible a_0–f_0 mixing phenomenon. Especially we would like to get a first quantitative understanding of the possible impact of isospin-violating couplings. To do so we employ the chiral unitary approach, in which we will now include isospin-violating effects to leading order in chiral perturbation theory (ChPT) in both the strong and the electromagnetic sector. This allows us to address the following issues:

(1) Does the enhancement of isospin violation in the effective couplings near the $K\bar{K}$ thresholds, see Eq. (3), lead to similarly sizable effects as the kaon mass differences?
(2) What is the effect of soft photon exchange on the mixing amplitude, see Fig. 3?
(3) What is the resulting mass dependence of the signal for the mixing?
(4) In Refs. [20,21] it was claimed that, in the mass range considered, a_0–f_0 mixing is the by far dominant isospin-violating effect as it emerges from the overlap of two narrow resonances with very nearby masses. This issue is discussed in Sec. III B. As we will see, we are now in the position to check this estimate within a dynamical approach for a specific reaction.

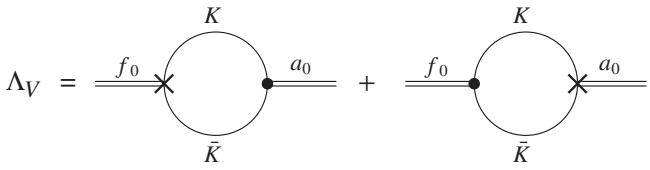

FIG. 2. Graphical illustration of the subleading contribution to the a_0–f_0 mixing matrix element Λ_V defined in Eq. (3). The crosses denote isospin-violating vertices.

For our calculations we use the chiral unitary approach as developed in Refs. [14,22], which provides the amplitudes for the scattering of two pseudoscalars from the coupled channel unitarization of the leading-order chiral Lagrangian. What is interesting about this approach is that it is not only able to describe the data on pseudoscalar-pseudoscalar S-wave scattering up to 1.2 GeV remarkably well, with just one cutoff of natural size, but also to dynamically generate the poles associated with the lightest scalar mesons without the need to introduce them explicitly in the Lagrangian. Hence, one can avoid *a priori* assumptions about the nature or even the existence of those resonances that come out naturally as a consequence of chiral symmetry and coupled channel unitarity. This reduces the model dependence of the approach considerably. In order to establish the nature of the generated poles, additional theoretical information is necessary, e.g. in Ref. [6] the leading $1/N_c$ behavior was used to provide evidence for a non-$q\bar{q}$ nature of the scalars. The scattering amplitudes obtained this way have then been used to implement the final-state interaction in the next-to-leading-order calculation of scalar form factors [23,24].

Another relevant aspect of unitarized ChPT is that it can be extended to higher orders, and, indeed, it is also possible

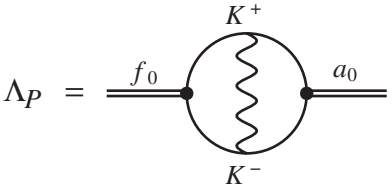

FIG. 3. Soft photon-exchange contribution to the a_0–f_0 mixing amplitude.

[1]By common isospin-breaking effects, we refer to those effects that occur at the Lagrangian level.

to use the fully renormalized next-to-leading-order unitarized ChPT scattering amplitudes [25–28] to match the final-state interactions into form factors [29]. However, for the scalar form factors we are interested in, it is possible to simplify the approach by matching their next-to-leading-order calculations just with the leading-order chiral unitary scattering amplitudes. Indeed, it has been shown [23,24] that this approximation already provides a very good description of the existing data on isospin-conserving processes, and thus provides a well founded starting point for our approach.

In the literature various reactions are discussed that should be sensitive to the isospin-violating a_0–f_0 mixing; amongst those are $\gamma p \to p\pi^0\eta$ [30], $\pi^- p \to \pi^0\eta n$ [31,32], $pn \to d\pi^0\eta$ [33–35], $dd \to \alpha\pi^0\eta$ [36], and $J/\Psi \to \phi\pi^0\eta$ [37,38]. In the first three certain differential observables are sensitive to a_0–f_0 mixing, for the last two the cross section is proportional to the square of the mixing amplitude, since the corresponding amplitudes vanish in the isospin limit. In this paper we will focus on the last reaction since the recent measurement by the BES collaboration of the isospin-conserving channel $J/\Psi \to \phi\pi^+\pi^-$ [39] shows a very pronounced signal of the f_0.[2] In addition, these data were already analyzed within the unitarized chiral approach in Ref. [24], going back to the formalism developed in Ref. [23], which is very convenient for our purposes since it determines the isospin-conserving part of our formalism rather accurately. A variant of this analysis, including isospin-breaking sources, forms the basis of our study.

II. THEORETICAL FRAMEWORK FOR THE ISOSPIN-CONSERVING CASE

A. Isospin states and scalar form factors

In all reactions listed above, where signals of a_0–f_0 mixing are expected, there are three strongly interacting particles in the final state. In principle, this necessitates a full three-body treatment using relativistic Faddeev equations. However, since we will focus on a phenomenon that occurs within a very narrow kinematic window, we will adopt the usual approximation that kinematics can be chosen such that the interactions within the particle pair of interest can be isolated. This approximation has already been demonstrated to provide a good description of the data [23,24], but should be checked within a Dalitz plot analysis of the data, once available.

Therefore, in what follows we assume that only the interaction of the two outgoing pseudoscalar particles needs to be considered. The full production amplitude is then given by the scalar form factor times at most a polynomial [40]. Since we are interested in a phenomenon that occurs within a mass range of a few tens of MeV only, we can safely use a polynomial of zeroth order only.

The considerations above are rather general and should hold for all reactions listed above as possible candidates to find signals of a_0–f_0 mixing. As a concrete example and since it will be used below, we now briefly reiterate the formalism of Refs. [23,24] to describe the decay of the J/Ψ into a ϕ and two pseudoscalars. We use a Lagrangian coupling the two vector particles to scalar currents of zero isospin in the form

$$\mathcal{L} = C_\phi \Psi^\mu \phi_\mu [\bar{s}s + \lambda_\phi \bar{n}n], \tag{5}$$

where $\bar{n}n = (\bar{u}u + \bar{d}d)/\sqrt{2}$. The two parameters C_ϕ, λ_ϕ are *a priori* unknown and have been extracted by fits to experimental data in Refs. [23,24]. Note that these analyses assume λ_ϕ to be *real*, which amounts to neglecting left-hand cuts or crossed-channel final-state interactions (the latter can in principle be separated in a careful analysis of the Dalitz plot). The matrix element for the full decay then involves matrix elements of the scalar currents between the vacuum and two pseudoscalars, which are described by scalar form factors as follows:

$$\begin{aligned} -\sqrt{2}B\Gamma^n_\pi(s) &= \langle 0|\bar{n}n|\pi\pi\rangle_{I=0}, \\ -\sqrt{2}B\Gamma^n_K(s) &= \langle 0|\bar{n}n|K\bar{K}\rangle_{I=0}, \\ -\sqrt{2}B\Gamma^n_\eta(s) &= \langle 0|\bar{n}n|\eta\eta\rangle_{I=0}, \end{aligned} \tag{6}$$

and equivalent definitions of the strange scalar form factors with the replacements $\bar{n}n \to \bar{s}s$, $\Gamma^n_i \to \Gamma^s_i$. The connection of the two-meson states of definite isospin to the basis of physical particles is given in Appendix A.

B. Form factors and unitarization

Using ChPT to a certain (e.g. next-to-leading) order to calculate the form factors defined in Eq. (6) guarantees that we obtain a consistent low-energy expansion, with the correct chiral loop corrections. However, we are interested in the energy region of the a_0 and f_0 resonances, which is outside the realm of applicability of ChPT amplitudes. The latter are, up to branch cuts generated by Goldstone boson dynamics, just polynomials in energy, and as such cannot generate the poles that quantum field theory requires to be associated with resonances. In addition, these polynomials will grow with energy and severely violate the unitarity bounds.

It is, however, well known that the two caveats above can be fixed by the unitarization of the ChPT amplitudes [14,22,25–28,41–43]. In practice, one first unitarizes the partial waves of definite angular momentum J for the scattering of two pseudoscalars, which generates the poles associated to the $a_0(980)$ for isospin $I = 1$ and $f_0(980)$ for isospin $I = 0$ [the latter together with the $f_0(600)$, which is

[2] In principle, one could also study $J/\Psi \to \omega\pi^0\eta$; however, there is no clear signal of the f_0 visible in the corresponding isospin-conserving channel $J/\Psi \to \omega\pi\pi$, and therefore also no pronounced mixing amongst a_0 and f_0 should be expected in this channel.

of little relevance in the context of this article]. These unitarized scattering amplitudes are then matched to the form factors in such a way that the latter have the same poles as the scattering amplitudes, and therefore the same resonances. They do not grow with energy either and satisfy Watson's theorem of final-state interactions.

Let us briefly review the general formalism before introducing the necessary modifications for the subsequent inclusion of isospin breaking. Assuming that only two-body intermediate states are relevant for the process, the unitarity conditions for the T-matrix, once projected onto partial waves of definite angular momentum J (see Appendix D), read

$$\mathrm{Im}\, T(s) = T(s)\Sigma(s)T^*(s), \tag{7}$$

$$\mathrm{Im}\, \Gamma(s) = T(s)\Sigma(s)\Gamma^*(s), \tag{8}$$

where

$$T(s) = \begin{pmatrix} T_{11}(s) & T_{12}(s) & T_{13}(s) \\ T_{12}(s) & T_{22}(s) & T_{23}(s) \\ T_{13}(s) & T_{23}(s) & T_{33}(s) \end{pmatrix},$$
$$\Gamma(s) = \begin{pmatrix} \Gamma_1(s) \\ \Gamma_2(s) \\ \Gamma_3(s) \end{pmatrix}, \tag{9}$$
$$\Sigma(s) = \frac{1}{16\pi} \begin{pmatrix} \sigma_1(s) & 0 & 0 \\ 0 & \sigma_2(s) & 0 \\ 0 & 0 & \sigma_3(s) \end{pmatrix},$$

and $T_{ij}(s)$ is the partial wave T-matrix with angular momentum J of the scattering between states i and j. The $\sigma_i(s) = 2k_i/\sqrt{s}$ account for the phase space of the intermediate two-body states, where k_i is the center-of-mass momentum of each physically accessible state i.

For illustration we have explicitly written the equations for three coupled states $i, j = 1, 2, 3$, because in the problem at hand, the $I = 0$ and $J = 0$ isospin-conserving process corresponds to this formalism with the identification $1 = \pi\pi$, $2 = K\bar{K}$, $3 = \eta\eta$, and the Γ_i are just the form factors defined in Eq. (6) above. Nevertheless, in Refs. [23,24] the calculations were performed in a two-channel approach neglecting the final-state effects of $\eta\eta$ rescattering, which will be included here for completeness (and consistency). Let us remark, finally, that the above formulas as well as the following results in this section are ready for a straightforward generalization to the case when the isospin states mix. In particular, we will have to deal with six coupled channels once we introduce isospin violation in the next sections.

As explained above, the ChPT partial wave T-matrices and form factors cannot satisfy Eqs. (7) and (8). Let us remark that Eq. (7) implies that $T(s)^{-1} = \mathrm{Re}T^{-1}(s) - i\Sigma(s)$, so that, indeed, we only have to find an approximation to $\mathrm{Re}T^{-1}$. Actually, partial waves satisfying the coupled channel unitarity constraint are obtained from the following expression [14,22]:

$$T(s) = [I - T^{(2)}(s)G(s)]^{-1}T^{(2)}(s), \tag{10}$$

where I is the identity matrix, $T^{(2)}$ is the leading-order ChPT T-matrix, $T = T^{(2)} + \mathcal{O}(p^4)$, and $G(s)$ is a diagonal matrix whose elements $G_i(s)$ are one-loop integrals corresponding to the two mesons of the state i propagating in the loop; detailed expressions are provided in Appendix B. Note that, in the physical (or charge) basis, $G(s)$ is a matrix whose diagonal elements $G_i(s)$ are analytic functions except for a right cut starting at each i state threshold. The imaginary part of $G_i(s)$ is precisely $\sigma_i(s)/16\pi$. Moreover, if T is reexpanded, one recovers the leading-order ChPT result including the correct imaginary part obtained at one loop. In addition, the factor $[I - T^{(2)}G(s)]^{-1}$ generates the required poles associated with resonances. Alternative derivations of this unitarization formalism make use of Lippmann-Schwinger-like equations [14] or dispersive approaches [25–27].

Unitarization thus provides the summation of the two-meson s-channel loops, since the $G(s)$ functions yield the correct imaginary part and a cutoff that can be fixed to approximate the real part of $\mathrm{Re}T^{-1}$, effectively absorbing higher-order terms. This has been shown to be sufficient to reproduce the available scattering data on the scalar channel and generates the observed resonances [14,22]. Of course, with one natural cutoff this approximation is not always valid over the whole light resonance regime, and indeed next-to-leading-order terms are necessary to generate other states, like vectors, from unitarization [25–27].

Equation (10) shows how to unitarize scattering amplitudes, but starting from this expression it is straightforward to also obtain scalar form factors that satisfy Eq. (8), writing [23]

$$\Gamma(s) = [I - T^{(2)}(s)G(s)]^{-1}R(s), \tag{11}$$

where $R(s)$ is a vector of real functions free from any singularity, which can be determined from a matching to the next-to-leading-order ChPT calculation of the form factors $\Gamma = \Gamma^{(0)} + \Gamma^{(2)} + \mathcal{O}(p^4)$ [44]. By reexpanding $[I - T^{(2)}(s)G(s)]^{-1} \simeq I + T^{(2)}(s)G(s) + \cdots$, one can extract $R(s)$ from

$$\Gamma(s) = [I + T^{(2)}G(s)]R(s) + \mathcal{O}(p^4). \tag{12}$$

Since the $G(s)$ integrals do have a residual cutoff q_{max} dependence, not present in the renormalized next-to-leading-order ChPT calculation of Γ, this matching has to be performed at a given renormalization scale $\mu = 1.2q_{\mathrm{max}}$ [see [22] for the relation between the cutoff and dimensional regularization of the $G(s)$ functions]. We provide the explicit expressions for $R(s)$ in Appendix C. We will now discuss how this formalism needs to be extended to include the effects of isospin violation.

III. ISOSPIN VIOLATION, THEORETICAL FRAMEWORK

Let us focus on the production reaction $J/\Psi \to \phi\pi^0\eta$, and calculate the matrix element

$$\mathcal{M}_{\phi}^{\pi\eta} = C_\phi \langle 0|\bar{s}s + \lambda_\phi \bar{n}n|\pi^0\eta\rangle. \tag{13}$$

In analogy to what we described above for the isospin-conserving case, the matrix element will be written in terms of scalar form factors

$$\begin{aligned} -\sqrt{2}B\Gamma^n_{\pi\eta}(s) &= \langle 0|\bar{n}n|\pi^0\eta\rangle, \\ -\sqrt{2}B\Gamma^s_{\pi\eta}(s) &= \langle 0|\bar{s}s|\pi^0\eta\rangle, \end{aligned} \tag{14}$$

which obviously vanish in the isospin limit, as the source terms are isoscalar, while the final state has $I = 1$. We will start with a variant of the recent analysis of the reaction $J/\Psi \to \phi\pi^+\pi^-$ [24]. There the data reported by the BES collaboration [39] was analyzed using the same unitarized chiral approach, sketched in the previous section, for the meson-meson final-state interaction. Thus, all that needs to be done to investigate the effect of isospin violation is to replace the matrix $G(s)$, the vector $R(s)$, and the meson-meson scattering matrix used there by those including isospin violation.

A. Form factor unitarization with isospin violation

Unitarization does not actually rely on isospin conservation, but is just a formalism derived for partial waves that could have been applied equally well in the physical (charge) instead of the isospin basis, which is indeed the most appropriate, once we allow for isospin breaking. Isospin-breaking effects in unitarized chiral effective theories have been studied before in the context of η and η' decays, see Refs. [45,46].

The enhancement of isospin violation we are interested in is due to the fact that we are looking at the region of the two $K\bar{K}$ thresholds, where the dynamics is dominated by the resonances already generated within the chiral unitary approach. Isospin breaking is a small correction to the isospin-conserving formalism, which simply amounts to increasing the number of distinct states and to slightly modifying the structure of the vertices.

In the following sections, we will thus perform the calculation of the different pieces needed in order to include isospin violation in the chiral unitary approach to the scalar form factors, as described in Sec. II B. In particular, in addition to the three $I = 0$ states, we now also have to consider two $I = 1$ and one $I = 2$ states. Hence, the $T^{(2)}$ matrix is now six dimensional, and its elements are easily obtained from the partial waves, shown in Appendices A and D. The matrix of loop functions is also six-dimensional, as seen in Eq. (22).

We can obtain all unitarized form factors for J/Ψ decays into a ϕ plus two S-wave pseudoscalar mesons in the isospin basis from the following equation:

$$\begin{pmatrix} \Gamma^{I=2}_{\pi\pi}(s) \\ \Gamma^{I=0}_{\pi\pi}(s) \\ \Gamma^{I=0}_{\eta\eta}(s) \\ \Gamma^{I=0}_{K\bar{K}}(s) \\ \Gamma^{I=1}_{K\bar{K}}(s) \\ \Gamma^{I=1}_{\pi\eta}(s) \end{pmatrix} = [I - T^{(2)}(s)G(s)]^{-1} \begin{pmatrix} 0 \\ R^s_\pi(s) + \lambda_\phi R^n_\pi(s) \\ R^s_\eta(s) + \lambda_\phi R^n_\eta(s) \\ R^s_K(s) + \lambda_\phi R^n_K(s) \\ \tilde{\lambda}_\phi R^{ud}_K(s) \\ R^s_{\pi\eta}(s) + \lambda_\phi R^n_{\pi\eta}(s) + \tilde{\lambda}_\phi R^{ud}_{\pi\eta}(s) \end{pmatrix}, \tag{15}$$

where all the R functions can be found in Appendix C and in Eqs. (25) and (36). The $I = 1$ polynomial form factor terms $\propto \tilde{\lambda}_\phi$, as well as the appearance of $I = 0$ form factors $R^{n,s}_{\pi\eta}(s)$ in the $\pi\eta$ channel will be discussed in detail in Sec. III F. We neglect an isospin-violating production vertex with $I = 2$ since it would be subleading in $m_d - m_u$. Similarly, contributions $\propto \tilde{\lambda}_\phi R^{ud}_{\pi,K,\eta}(s)$ could be added to the $I = 0$ production terms, but are neglected as second order in isospin violation. Let us remark that, if we turn off isospin violation in $T^{(2)}$ and $G(s)$ and set $\tilde{\lambda}_\phi = 0$, $R^n_{\pi\eta}(s) = R^s_{\pi\eta}(s) = 0$, we recover the three coupled channel isospin-conserving case.

For the study of a_0–f_0 mixing, we are interested in the $I = 1$ form factors and more precisely in $\Gamma^{I=1}_{\pi\eta}(s)$ in the region around the $K\bar{K}$ threshold. Note that Eq. (15) is very convenient in order to switch on and off the different contributions to isospin violation, and study their sizes, since all the isospin violation in vertices appears in $T^{(2)}$, and the difference between charged and neutral loops appears in $G(s)$. This will be studied in Sec. IV.

B. Why a_0–f_0 mixing should dominate isospin violation

In Refs. [20,21], it was claimed that, if the invariant mass of the outgoing two-meson pair is close to the nominal mass of both f_0 and a_0, then the mixing of the two should be, by far, the dominant isospin-violating effect. The argument was based on the fact that the two scalar resonances of interest are narrow and overlap and therefore the effect of isospin violation as it occurs in the propagation of the scalar mesons is enhanced compared to mixing in the production operator. In Refs. [20,21], the reasoning

was presented for NN induced production of the scalar mesons. Here we adopt it for J/Ψ decays. For the sake of this argument only, we introduce the notion of explicit resonance (a_0, f_0) propagators; we emphasize, though, that such objects never appear in this form in our unitarized chiral amplitudes, where the corresponding poles are generated dynamically.

We expect the effect of isospin violation in the production operator [$\propto \tilde{\lambda}_\phi$ in Eq. (15)] to scale at most as $(m_d - m_u)/m_s$. This is then followed by an isospin-conserving final-state interaction proportional to $W_{a_0\to\pi\eta}G_{a_0}$, where G_{a_0} denotes the a_0 propagator and $W_{a_0\to\pi\eta}$ the a_0 decay matrix element—if we assume a scalar coupling of the a_0 to $\pi\eta$, the vertex function $W_{a_0\to\pi\eta}$ reduces to the effective coupling constant $g_{a_0\pi\eta}$ [cf. the corresponding couplings to the kaon channels defined in Eq. (1)]. On the other hand, a_0–f_0 mixing occurs in the propagation, here parametrized by the various isospin-violating scalar form factors $\Gamma^{n,s}_{\pi\eta}$. We may therefore use

$$\Gamma^{n,s}_{\pi\eta} \sim W_{a_0\to\pi\eta}G_{a_0}\Lambda G_{f_0}. \tag{16}$$

Here Λ denotes the mixing matrix element, see Eq. (4). As it has been argued in the Introduction, Λ scales as $M_K^2\sqrt{(m_d - m_u)/m_s}$. For the f_0 propagator very close to the $K\bar{K}$ threshold, we may use

$$G_{f_0} = \frac{1}{s - m_{f_0}^2 + i m_{f_0}\Gamma_{f_0}}, \tag{17}$$

which reduces to $-i/(m_{f_0}\Gamma_{f_0})$ for $s \simeq m_{a_0}^2 \simeq m_{f_0}^2$. Thus, the ratio of the two effects, and therefore an estimate of the theoretical uncertainty of the investigation, is given by $m_{f_0}\Gamma_{f_0}\sqrt{(m_d - m_u)/m_s}/M_K^2$, which is of the order of 4% for the amplitude (for this estimate we used 50 MeV for the width). This estimate can now be tested within a dynamical approach.

C. Lagrangians, mass splittings, etc.

We use the leading-order chiral Lagrangian $\mathcal{L}^{(2)}$ including isospin-breaking/electromagnetic effects [47]:

$$\mathcal{L}^{(2)} = \frac{F^2}{4}\langle D_\mu U D^\mu U^\dagger + \chi U^\dagger + U\chi^\dagger\rangle + C\langle QUQU^\dagger\rangle. \tag{18}$$

U collects the Goldstone boson fields in the usual manner, F is the common pseudoscalar meson decay constant. The covariant derivative, in particular, contains the coupling to photons, $D_\mu U = \partial_\mu U - iQ[A_\mu, U] + \cdots$, and Q is the quark charge matrix, $Q = e\,\mathrm{diag}(2, -1, -1)/3$. The field χ collects the quark masses, $\chi = 2B\,\mathrm{diag}(m_u, m_d, m_s) + \cdots$. We choose to express isospin-breaking effects due to the light quark mass difference in terms of the leading order $\pi^0\eta$ mixing angle

$$\epsilon = \frac{\sqrt{3}}{4}\frac{m_d - m_u}{m_s - \hat{m}} + \mathcal{O}((m_d - m_u)^3). \tag{19}$$

Electromagnetic contributions $\propto C$ in Eq. (18) can be reexpressed in terms of the charged-to-neutral pion mass difference,

$$\Delta_\pi = M_{\pi^+}^2 - M_{\pi^0}^2 = \frac{2Ce^2}{F^2}, \tag{20}$$

where the tiny strong mass difference $\propto (m_d - m_u)^2$ is neglected. Because of Dashen's theorem, the charged-to-neutral kaon mass difference can then be written at leading order as

$$\Delta_K = M_{K^+}^2 - M_{K^0}^2 = \Delta_\pi - \frac{4\epsilon}{\sqrt{3}}(M_K^2 - M_\pi^2). \tag{21}$$

As outlined in the Introduction, the meson mass differences, especially those of the kaons, naturally introduce a striking isospin-violating effect. Note that, as a consequence of the previous arguments, the matrix of loop functions $G(s)$ is now six dimensional, i.e. is diagonal in the charge basis

$$G = \mathrm{diag}(G_{\pi^+\pi^-}, G_{\pi^0\pi^0}, G_{\eta\eta}, G_{K^+K^-}, G_{K^0\bar{K}^0}, G_{\pi^0\eta}), \tag{22}$$

but has only a block-diagonal form in the isospin basis (see Appendix A).

We have pointed out in Eq. (1) that the mass difference in the kaon propagators generates the leading isospin-breaking contribution in the a_0/f_0 resonance region. As we are about to calculate subleading isospin-violating effects, one may wonder how accurately the unitarity cut contribution is described by the (leading-order) chiral unitary approach, and how much this description would change if we considered unitarized chiral p^4 amplitudes (see Refs. [25–27]). In this formalism we do not introduce the couplings of the a_0 and f_0 to different isospin channels explicitly, which, as seen in Eq. (1), determine the strength of the leading part of the mixing amplitude. Actually, within this approach, those couplings correspond to the residues of the poles that have been generated dynamically when fitting the data. In this sense the couplings are determined by the set of data that has been fitted to obtain the isospin-conserving part. The formalism as presented is very general and for the S-waves, the quality of such fits depends mainly on the data considered, and hardly changes with the order of the unitarized chiral amplitudes. Of course, whenever new data appears for the isospin-conserving reactions, the corresponding parts can be refitted and therefore allow for an improvement in the accuracy also for the isospin-violating amplitudes. However, the relevant observation is that at any time the possible effect of isospin violation in the couplings, as discussed in the following section, should be considered.

D. Isospin violation in vertices

Isospin violation in the Lagrangian in Eq. (18) does not only induce charged-to-neutral pion and kaon mass differences, but also affects the (tree-level) scattering amplitudes, which receive corrections to their isospin-conserving expressions. This formalism allows one to calculate isospin violation in scattering consistently with the analysis of the masses. A well-known example for the importance of such effects is the sizable correction in relating $\pi\pi$ scattering amplitudes at threshold to the isospin scattering lengths [48]; similar corrections have also been calculated e.g. in πK scattering [49–52]. In addition, some transitions only take place at all in the presence of isospin violation, the most prominent being the decay $\eta \to 3\pi$ [53,54].

The isospin-violating scattering T-matrix has to be calculated in the particle or charge basis; the complete list of amplitudes, linking all charge- and strangeness-neutral channels, calculated at leading order within ChPT, i.e., $T \simeq T^{(2)} + \mathcal{O}(p^4)$, is given in Appendix D. Note that we now have six coupled states, but as we have commented in Sec. II B, the same unitarization formalism applies. Despite obtaining our calculations in the charge basis, it is still convenient to recast them in the isospin basis, as we assume (for the moment) production of a pure $I = 0$ state, while $\pi^0\eta$ is $I = 1$. We show its relation to the charge basis in Appendix A. Obviously, the matrix of scattering amplitudes in the isospin basis is not block diagonal with respect to $I = 0, 1, 2$ anymore, but allows for transitions between different isospin quantum numbers; these transition matrix elements scale with either ϵ or e^2.

In the resonance picture of Eqs. (1) and (3), isospin violation in the meson-meson vertices induces the isospin-violating resonance couplings $g^I_{RK\bar{K}}$. As we have no strict counting scheme for energies in the resonance region, these resonance couplings are only modeled this way, and may receive corrections from higher orders, although one should take into account that unitarization is necessarily taming their effect. They are not fixed by isospin-symmetric data in the way the cut contribution due to kaon mass differences are, and therefore have to be pinned down directly from isospin-violating decays, like the one discussed here.

E. Coulomb corrections

So far, all interaction terms derived from Eq. (18), entering the matrix $T^{(2)}$ in the unitarized final-state interaction, are pointlike four-meson vertices. We note, however, that Eq. (18) generates another tree-level diagram contributing to meson-meson scattering, namely, one-photon exchange between charged mesons. It is obvious that this nonlocal interaction cannot be taken into account on quite the same footing.

As all initial- and final-state particles in the decay $J/\Psi \to \phi\pi^0\eta$ are electrically neutral, photons can only enter inside charged-meson loops. The diagram shown in Fig. 4 is the only one at $\mathcal{O}(\alpha)$ that is enhanced at the K^+K^- threshold; we neglect all other, nonenhanced diagrams. Our prescription is then to replace the charged-kaon loop function $G_{K^+K^-}(s)$ in the unitarization sum by the sum of this and the one-photon exchange graph,

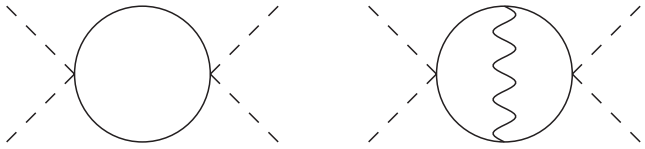

FIG. 4. Photon-exchange diagram that generates a singular behavior at the K^+K^- threshold (right). The full lines denote charged kaons, dashed lines arbitrary other mesons, and the wiggly line the exchanged photon. This is added to the standard K^+K^- one-loop function (left) in the iterated bubble sum.

$$G_{K^+K^-}(s) \to G_{K^+K^-}(s) + G^{1-C}_{K^+K^-}(s). \tag{23}$$

In the threshold region, the exact expression for the one-photon-exchange diagram [55] can well be approximated by the threshold-expanded form [56], which reads

$$G^{1-C}_{K^+K^-}(s) = \frac{\alpha}{32\pi}\left\{\log\frac{|s-4M^2_{K^+}|}{M^2_{K^+}} + \log 2 + \frac{21\zeta(3)}{2\pi^2} - i\pi\theta(s-4M^2_{K^+})\right\} + \mathcal{O}((s-4M^2_{K^+})^{1/2}). \tag{24}$$

A justification for this being the leading threshold behavior can also be given in the framework of a nonrelativistic theory [57].

We neglect exchange of multiple photons inside the meson bubble, although these are in principle also enhanced close to threshold. A resummation of multiphoton exchange is necessary once the parameter

$$\frac{\alpha}{2}\left(1 - \frac{4M^2_{K^+}}{s}\right)^{-1/2}$$

is not small anymore; it, e.g., becomes as large as 0.1 for $\sqrt{s} = 2M_{K^+} \pm 0.7$ MeV. The size of the more-than-one-photon exchange amplitude relative to one-photon one stays below 5% outside a window of ± 5 MeV around the charged-kaon threshold. As the energy resolution for potential experiments is expected to be of this order at best, neglecting higher-order photon graphs seems well justified. This is in line with the findings of Ref. [58].

Note that we only take photon exchange into account for the charged *kaon* loop graphs. We have checked that the corresponding modification inside the charged pion loops leads to no visible modification in the physical region of the process under investigation, i.e. above $\pi^0\eta$ threshold, and, in particular, not in the energy region around $K\bar{K}$ threshold considered here.

F. Isospin-violating production operators

It has been argued in Sec. III B that isospin violation in the final-state interaction ought to be the dominant effect for the production of the $\pi^0\eta$ final state in the energy region around the $K\bar{K}$ threshold. We can check this assumption explicitly by allowing for isospin breaking in the production operator. This occurs in two forms: due to mixing, the $\pi^0\eta$ final state has an $I = 0$ component, i.e. nonvanishing form factors with the $\bar{n}n$ and $\bar{s}s$ currents that scale with the mixing angle ϵ exist already at tree level; and we may allow for an additional $I = 1$ component in the scalar source terms given in Eq. (5).

1. Isospin-violating scalar form factors at tree level

The mixing of π^0 and η leads to nonvanishing form factors $\Gamma^{n,s}_{\pi\eta}(s)$ already at tree level. At leading order in the chiral expansion, where the propagators for π^0 and η can be diagonalized with a single mixing angle ϵ, the matrix element $\langle 0|\bar{u}u + \bar{d}d + \bar{s}s|\pi^0\eta\rangle$ has to vanish, leading to the relation $\sqrt{2}\Gamma^n_{\pi\eta}(s) + \Gamma^s_{\pi\eta}(s) = 0$. We find

$$R^n_{\pi\eta}(s) = -\frac{1}{\sqrt{2}} R^s_{\pi\eta}(s) = \frac{2}{3}\epsilon + \mathcal{O}(\epsilon^3), \tag{25}$$

as $\Gamma(s) = R(s) + \mathcal{O}(p^2)$, see Eq. (12). These components are added to the vector of production operators R of Eq. (15). In contrast to the $I = 1$ scalar source term discussed below, this effect does not induce any additional uncertainty, but comes with a fixed coefficient.

In principle, the task of this investigation consists precisely in the determination of the form factors $\Gamma^n_{\pi\eta}(s)$, $\Gamma^s_{\pi\eta}(s)$, and $\Gamma^{ud}_{\pi\eta}(s)$. In contrast to what was done in the isospin-conserving case, however, we only match the ChPT expressions for these form factors at leading order.

2. $I = 1$ scalar source term

We first introduce an $I = 1$ scalar source, generalizing the Lagrangian in Eq. (5) to

$$\mathcal{L} = C_\phi \Psi^\mu \phi_\mu [\bar{s}s + \lambda_\phi \bar{n}n + \frac{\tilde{\lambda}_\phi}{\sqrt{2}}(\bar{u}u - \bar{d}d)]. \tag{26}$$

In order to obtain an order-of-magnitude estimate of the size of the new parameter $\tilde{\lambda}_\phi$, we invoke a version of vector-meson dominance: we assume the dominant (isospin-conserving) production of a ρ^0 in association with the operator $(\bar{u}u - \bar{d}d)/\sqrt{2}$, with subsequent $\rho^0 - \phi$ mixing; see Fig. 5. Following Ref. [24], we write the interaction Lagrangian in the form

$$\mathcal{L} = g\Psi^\mu \left\{ \langle V_\mu \tilde{S}\rangle + \frac{\nu}{3}\langle V_\mu\rangle\langle S\rangle \right\}, \tag{27}$$

where V_μ collects the vector-meson fields, S is the matrix of scalar sources, and $\tilde{S} = S - \langle S\rangle/3$. Considering just the flavor-neutral vector mesons, we can rewrite Eq. (27) as

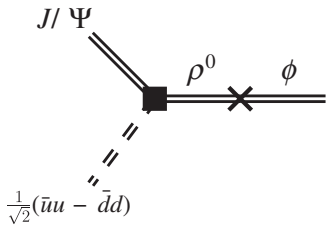

FIG. 5. Vector-meson mixing contribution to $\tilde{\lambda}_\phi$. The box denotes an (isospin-conserving) coupling of J/Ψ to ρ^0 and the $I = 1$ scalar source term, the cross the isospin-violating $\rho^0 - \phi$ mixing term.

$$\mathcal{L} = \Psi^\mu \Big\{ C_\phi \phi_\mu (\bar{s}s + \lambda_\phi \bar{n}n) + C_\omega \omega_\mu (\bar{s}s + \lambda_\omega \bar{n}n) + C_\rho \rho^0_\mu \frac{1}{\sqrt{2}}(\bar{u}u - \bar{d}d) \Big\}, \tag{28}$$

where C_ω, λ_ω, C_ρ can be expressed in terms of C_ϕ, λ_ϕ according to

$$C_\omega = \lambda_\phi C_\phi, \qquad \lambda_\omega = \frac{1}{\sqrt{2}} + \frac{1}{\lambda_\phi}, \qquad C_\rho = \left(1 - \frac{\lambda_\phi}{\sqrt{2}}\right) C_\phi. \tag{29}$$

$\rho^0 - \phi$ mixing is actually assumed to proceed via subsequent $\rho^0 - \omega$ and $\omega - \phi$ mixing. Neglecting the finite widths of the vector mesons, we find a coupling of the ϕ to the $(\bar{u}u - \bar{d}d)/\sqrt{2}$ operator in terms of the $\rho^0 - \omega$ and $\omega - \phi$ mixing angles $\Theta_{\rho\omega}$, $\Theta_{\omega\phi}$ of the form

$$C_\phi \tilde{\lambda}_\phi = C_\rho \frac{\Theta_{\rho\omega}\Theta_{\omega\phi}}{(M^2_\phi - M^2_\rho)(M^2_\phi - M^2_\omega)}, \tag{30}$$

and therefore

$$\tilde{\lambda}_\phi = \frac{\Theta_{\rho\omega}\Theta_{\omega\phi}}{(M^2_\phi - M^2_\rho)(M^2_\phi - M^2_\omega)}\left(1 - \frac{\lambda_\phi}{\sqrt{2}}\right). \tag{31}$$

Plugging in the central values for the mixing angles from Ref. [59], $\Theta_{\rho\omega} = -3.75 \times 10^{-3}$ GeV^2, $\Theta_{\omega\phi} = 25.34 \times 10^{-3}$ GeV^2, we obtain

$$\tilde{\lambda}_\phi \approx -0.5 \times 10^{-3}, \tag{32}$$

where the uncertainty due to errors in the input numbers is about 20%. It is interesting to note that a corresponding estimate based on $\omega - \phi$ mixing of the λ_ϕ parameter, which violates the Okubo-Zweig-Iizuka rule, would lead to

$$\lambda_\phi = \frac{\Theta_{\omega\phi}}{M^2_\phi - M^2_\omega} \approx 0.06, \tag{33}$$

which is only about a factor of 2 smaller than the fit result [24]. We therefore assume that the above order-of-magnitude estimate of $\tilde{\lambda}_\phi$ should be comparably accurate, and consider it a very conservative estimate to vary the

strength of the isospin-violating production operator within a range for $\tilde{\lambda}_\phi$ increased by a factor of ± 10 compared to Eq. (32).

In order to follow the formalism used earlier, we generalize the matrix element Eq. (13) to

$$\mathcal{M}_\phi^{\pi\eta} = C_\phi \langle 0|\bar{s}s + \lambda_\phi \bar{n}n + \frac{\tilde{\lambda}_\phi}{\sqrt{2}}(\bar{u}u - \bar{d}d)|\pi^0\eta\rangle, \quad (34)$$

and define the additional $I = 1$ scalar form factors Γ_K^{ud}, $\Gamma_{\pi\eta}^{ud}$ according to

$$\begin{aligned} -\sqrt{2}B\Gamma_K^{ud}(s) &= \left\langle 0 \left| \frac{1}{\sqrt{2}}(\bar{u}u - \bar{d}d) \right| K\bar{K} \right\rangle_{I=1}, \\ -\sqrt{2}B\Gamma_{\pi\eta}^{ud}(s) &= \left\langle 0 \left| \frac{1}{\sqrt{2}}(\bar{u}u - \bar{d}d) \right| \pi^0\eta \right\rangle_{I=1}. \end{aligned} \quad (35)$$

As we are only interested in an order-of-magnitude estimate for the effects of the $I = 1$ production operator, we refrain from doing the complete one-loop calculation of these form factors and only unitarize the lowest-order ($\mathcal{O}(p^2)$) results for these, which we find to be

$$R_K^{ud}(s) = \frac{1}{\sqrt{2}}, \qquad R_{\pi\eta}^{ud}(s) = -\frac{1}{\sqrt{3}} + \mathcal{O}(\epsilon^2). \quad (36)$$

We note that the Feynman-Hellman theorem implies the relation

$$\begin{aligned} R_{\pi\eta}^n(s) &= -\frac{1}{\sqrt{2}}R_{\pi\eta}^s(s) = -\frac{m_d - m_u}{2(m_s - \hat{m})}R_{\pi\eta}^{ud}(s) \\ &= \frac{2}{3}\epsilon + \mathcal{O}(\epsilon^3) \end{aligned} \quad (37)$$

at tree level, which can easily be checked to be fulfilled by Eqs. (25) and (36).

G. Further possible background terms

In Ref. [38], two candidates for background terms to an a_0–f_0 mixing description of the decay $J/\Psi \to \phi\pi^0\eta$ were estimated, namely $J/\Psi \to \gamma^* \to \phi\pi^0\eta$ and $J/\Psi \to (K^*\bar{K} + \text{H.c.}) \to \phi\pi^0\eta$. The former is clearly not covered by our description of this decay in terms of scalar form factors and would necessitate a generalization of the production mechanism beyond $\bar{q}q$ operators; luckily it was found to be much smaller than the signal and therefore will not be considered any further.

The latter, however, turned out to be of the order of or even larger than the signal and will now be discussed briefly. In the unitarized chiral approach, only the lightest pseudoscalar mesons appear as dynamical degrees of freedom. The effects of all other mesons, e.g. the K^*, are integrated out and are considered through local counterterms. The corresponding expressions can be deduced from those with dynamical heavy particles by formally taking the infinite mass limit.

According to Ref. [38] the transition in the decay chain $J/\Psi \to (K^*\bar{K} + \text{H.c.}) \to \phi a_0$ appears through a triangle loop that contains two kaon propagators and one K^* propagator; isospin violation then emerges through the kaon mass differences. In the effective theory description the vector-meson propagator needs to be replaced by a point interaction—as a result the whole transition is to be regarded as part of the isospin-violating scalar form factor and therefore, from our point of view, as part of the signal. In this sense it appears natural that the corresponding transition rate is of the order of the estimated signal.

IV. RESULTS AND DISCUSSIONS

The differential decay rate for the process $J/\Psi \to \phi\pi^0\eta$ is related to the absolute square of the matrix element

$$\mathcal{M}_\phi^{\pi\eta} = -\sqrt{2}BC_\phi[\Gamma_{\pi\eta}^s(s) + \lambda_\phi\Gamma_{\pi\eta}^n(s) + \tilde{\lambda}_\phi\Gamma_{\pi\eta}^{ud}(s)], \quad (38)$$

with the form factors $\Gamma_{\pi\eta}^s(s)$ $\Gamma_{\pi\eta}^s(s)$, and $\Gamma_{\pi\eta}^{ud}(s)$ given by the matrix relation Eq. (15), by

$$\frac{d\Gamma}{d\sqrt{s}} = \frac{\sqrt{\lambda(M_{J/\Psi}^2, s, M_\phi^2)\lambda(s, M_{\pi^0}^2, M_\eta^2)}}{16\sqrt{s}M_{J/\Psi}^2(2\pi)^3}F_{\text{pol}}|\mathcal{M}_\phi^{\pi\eta}|^2, \quad (39)$$

where $\lambda(x, y, z) = x^2 + y^2 + z^2 - 2(xy + xz + yz)$ is the usual Källén function, and F_{pol} is the kinematical factor that takes the average and sum over polarization states of J/Ψ and ϕ into account,

$$\begin{aligned} F_{\text{pol}} &= \frac{1}{3}\sum_{\rho,\rho'}\epsilon_\mu(\rho)\epsilon^\mu(\rho')\epsilon_\nu^*(\rho)\epsilon^{\nu*}(\rho') \\ &= \frac{2}{3}\left[1 + \frac{(M_{J/\Psi}^2 + M_\phi^2 - s)^2}{8M_{J/\Psi}^2M_\phi^2}\right]. \end{aligned} \quad (40)$$

The data for $J/\Psi \to \phi\pi^+\pi^-$ [39] analyzed in Ref. [24] do not provide normalized differential decay widths, but only event distributions, $dN/d\sqrt{s} \propto d\Gamma/d\sqrt{s}$, with an unknown constant of proportionality. Accordingly, we cannot predict a normalized differential decay width for $J/\Psi \to \phi\pi^0\eta$ either, but only a *relative* width, normalized by the isospin-conserving 2-pion decay channel. We choose to perform the normalization according to

$$\begin{aligned} &\frac{dN}{d\sqrt{s}}(J/\Psi \to \phi\pi^0\eta)\bigg|_{\text{norm}} \\ &= \frac{d\Gamma}{d\sqrt{s}}(J/\Psi \to \phi\pi^0\eta)\Big/\int_{W_1}^{W_2} d\sqrt{s}\frac{d\Gamma}{d\sqrt{s}}(J/\Psi \to \phi\pi^+\pi^-), \end{aligned} \quad (41)$$

where the energy range $W_{1,2} = 2M_{K^+}^2 \mp 25$ MeV covers the peak region of the a_0–f_0 mixing signal. The numerical input on masses and coupling constants that enter our calculations are given in Appendix E. We remark that the coupling constant C_ϕ as well as the form factor normal-

ization constant B, see Eq. (38), cancel out in the ratio in Eq. (41) and do not have to be specified in our analysis. We wish to emphasize that there are *no new* fit parameters in this analysis: the unitarization procedure in the chiral unitary approach at this order contains one single parameter, the cutoff $q_{\max}$, which has been adjusted as to reproduce the S-wave meson-meson scattering data in all physical channels (i.e., in particular, the resonance pole positions) as well as possible. All further parameters, both the parameter λ_ϕ in Eq. (5) as well as the $\mathcal{O}(p^4)$ chiral low-energy constants L_i^r in the various scalar form factors, only serve as a parametrization to describe the isospin-conserving $J/\Psi \to \phi\pi\pi$ data.

Of course, in order to predict realistic relative count rates, one would have to take into account different detector efficiencies for the two different final states, which we do not do here; it will be straightforward to implement them, once such experimental specifications become available.

As stated above, the $\pi^0\eta$ invariant mass distribution of the reaction $J/\Psi \to \phi\pi^0\eta$ is proportional to the absolute value squared of the mixing matrix element, at least as long as we do not include any isospin violation in the production operator. In Fig. 6 we show our prediction for the $\pi^0\eta$ invariant mass distribution when different isospin-violating effects are included in the propagation of the scalar mesons. To produce the dashed line only the kaon mass difference was included. The resulting curve is in qualitative agreement with those of Refs. [18,19]. Including isospin violation in the vertices, we find the dot-dashed curve; adding one-photon exchange according to Sec. III E leads to the full result, given by the solid line. We find that the effect of photon-exchange is rather small even in the threshold region, and certainly smaller than the modifications due to isospin violation in the meson-meson scattering vertices (for a more detailed study of photon effects see Ref. [58]). The signal for a_0–f_0 mixing is therefore significantly enhanced compared to the original estimate given in Ref. [18].

Next we investigate the possible effect of isospin violation in the production operator. As one can see in Fig. 7, in the region around the kaon threshold the invariant mass distribution in the $\pi^0\eta$ channel is by far dominated by the isospin violation in the propagation. The admixture of an isospin-violating production operator as estimated in Sec. III F actually produces only a rather narrow band very close to the result without such an operator. This nicely confirms the corresponding estimates provided in Refs. [20,21].

In order to demonstrate the enhancement of isospin-breaking in the two-kaon threshold region, as well as due to different mechanisms, we show the predicted event numbers in Table I, normalized to 1000 $J/\Psi \to \phi\pi^+\pi^-$ events in the peak region, for three distinct kinematical regions: for the two-kaon threshold region of total width

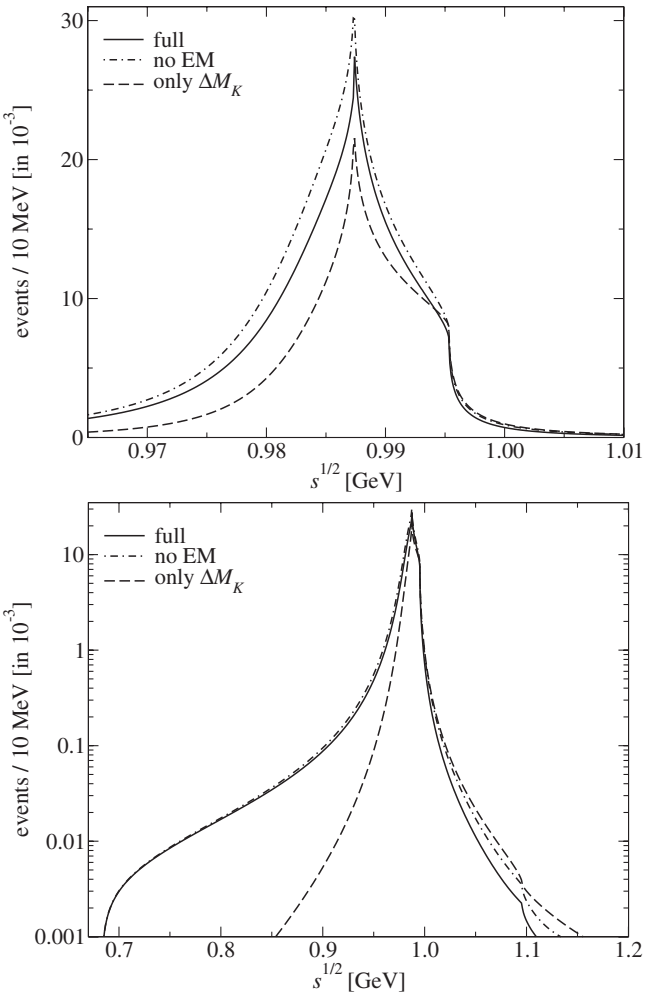

FIG. 6. Predictions for the normalized $J/\Psi \to \phi\pi^0\eta$ differential count rate per 10 MeV, relative to 1000 $J/\Psi \to \phi\pi^+\pi^-$ events in the peak region $2M_{K^+}^2 \pm 25$ MeV as defined in Eq. (41). We show the successive inclusion of the different isospin-violating effects in the final-state interaction. The kaon mass difference alone leads to the dashed line, additional inclusion of isospin violation in the strong vertices produces the dot-dashed curve. As the full result, adding one-photon-exchanges in the bubble sum, we obtain the solid curve. The top panel shows the most relevant region near the two $K\bar{K}$ thresholds; in order to make the enhancement in this region more obvious, the bottom panel shows the whole energy range from threshold up to 1.2 GeV on a logarithmic scale.

50 MeV, below down to $\pi^0\eta$ threshold, and above up to 1.2 GeV. We want to point out that the signal around 1 GeV is enhanced by nearly 50% compared to the original estimate based on the kaon mass difference effect alone. The reduction due to photon exchange visible in Fig. 6 is about 10%, the corresponding event number in region II of Table I without photon exchange would be 33.6. Obviously, all mechanisms other than the kaon mass difference also lead to a large relative increase of mixing *outside* this central region, in particular, the isospin-violating production operator; this is also clearly seen in

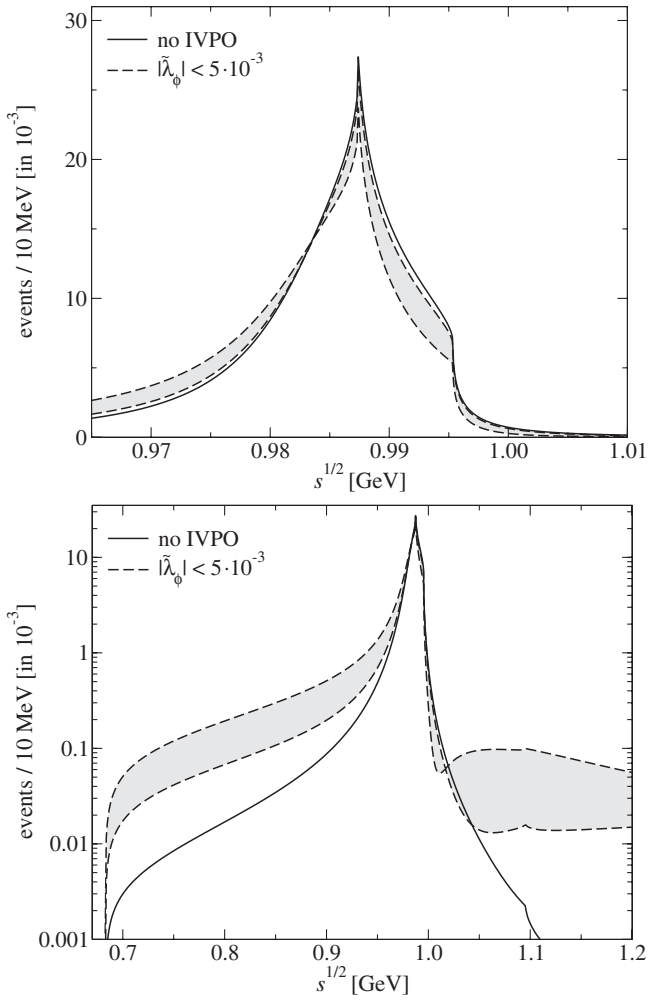

FIG. 7. Predictions for the $J/\Psi \to \phi\pi^0\eta$ differential count rate per 10 MeV (normalization as in Fig. 6), with (band) and without (full line) inclusion of an isospin-violating production operator (IVPO). The central curve is shifted by the isospin violation in the scalar form factors as discussed in Sec. III F 1, the band is due to the $I = 1$ scalar source with strength limited by $\tilde{\lambda}_\phi = \pm 5 \times 10^{-3}$, see Sec. III F 2. As in Fig. 6, the top panel shows the two-kaon threshold region, the bottom one the whole energy range from threshold up to 1.2 GeV on a logarithmic scale.

the logarithmic plots over a wider energy range in Figs. 6 and 7. However, a relative enhancement of the signal by more than 2 orders of magnitude close to the two-kaon thresholds remains. Finally, we wish to point out that 29.0 $J/\Psi \to \phi\pi^0\eta$ events in the resonance region relative to 1000 $J/\Psi \to \phi\pi^+\pi^-$ in the same kinematic range may look like a mere 3% effect of isospin violation, but, due to the lack of interference, it corresponds to about 17% isospin breaking on the amplitude level. Therefore, a_0–f_0 mixing leads indeed to a very sizable isospin-violating signal.

As a side remark, we briefly comment on the form factors $\Gamma^n_{\pi\eta}(s)$, $\Gamma^s_{\pi\eta}(s)$ individually, which in principle

TABLE I. Event estimates for $J/\Psi \to \phi\pi^0\eta$ for different energy regions and different isospin-breaking effects. The energy regions are: Region I: $M_{\pi^0} + M_\eta \le \sqrt{s} \le 2M_{K^+} - 25$ MeV; Region II: $2M_{K^+} - 25$ MeV $\le \sqrt{s} \le 2M_{K^+} + 25$ MeV; Region III: $2M_{K^+} + 25$ MeV $\le \sqrt{s} \le 1.2$ GeV. "ΔM_K" refers to the original estimate [18], assuming the kaon mass difference as the only source of a_0–f_0 mixing. "Full FSI" labels the model with all isospin-breaking effects in the final-state interaction (FSI) included, while "Including IVPO" also incorporates the isospin-violating production operators discussed in Sec. III F. All event numbers are relative to 1000 $J/\Psi \to \phi\pi^+\pi^-$ events in Region II.

	Region I	Region II	Region III
ΔM_K	0.3	20.3	0.7
Full FSI	2.4	29.0	0.4
Including IVPO	$7.2^{+3.3}_{-2.7}$	$28.2^{+0.6}_{-0.2}$	$0.6^{+1.0}_{-0.1}$

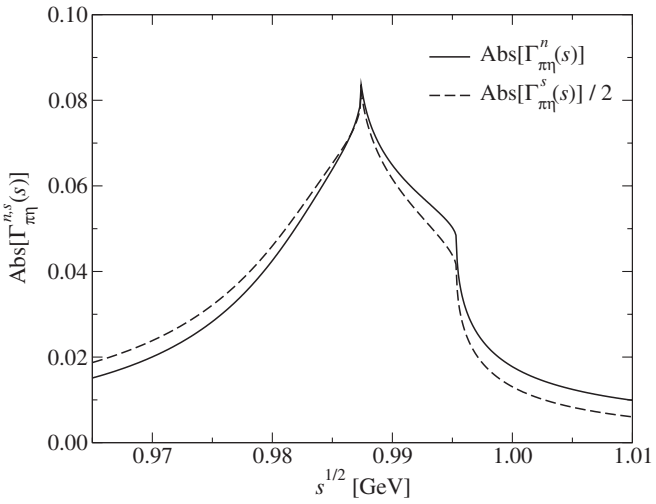

FIG. 8. Absolute values of the scalar form factors $\Gamma^n_{\pi\eta}(s)$ (full line), $\Gamma^s_{\pi\eta}(s)$ (dashed line). Note that, to facilitate the comparison, the latter has been scaled down by a factor of 2.

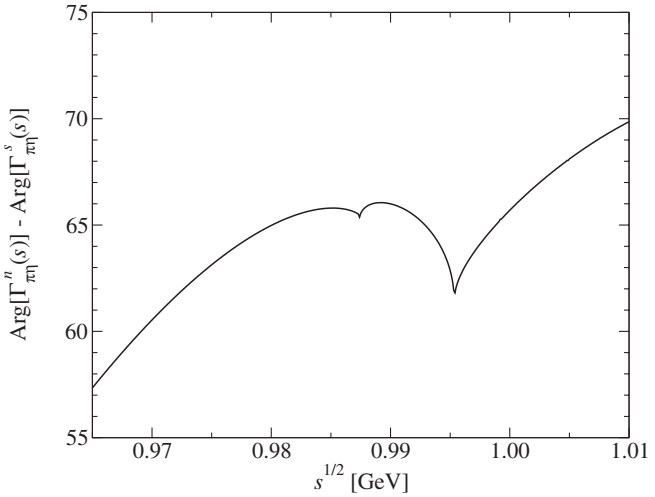

FIG. 9. Relative phase of nonstrange and strange $\pi\eta$ scalar form factors, $\mathrm{Arg}[\Gamma^n_{\pi\eta}(s)] - \mathrm{Arg}[\Gamma^s_{\pi\eta}(s)]$.

may occur in a different relative combination when a_0–f_0 mixing is investigated in the context of a different decay or production mechanism. In Figs. 8 and 9, we show the absolute values of the form factors as well as the *difference* of the phase motions of the two (both including all isospin-breaking mechanisms discussed earlier). We find that the shape of (the absolute values of) both form factors is very similar, and that the phase difference, while showing remnants of the cusps, varies rather mildly over the two-kaon threshold region (by altogether less than 15°). We conclude from these observations that, if the relative strength parameter λ_ϕ is replaced by a different, possibly complex (but still approximately constant) value, we would not expect the mixing signal to be wildly different from what we predict here.

V. SUMMARY

In this work we have improved the theoretical understanding of the phenomenon of a_0–f_0 mixing. We have confirmed that the dominant mixing effect comes from the kaon mass difference in line with Ref. [18]. It is therefore possible to extract independent information on the effective couplings of $a_0(980)$ and $f_0(980)$ to kaons, which contain important structure information [15], from the mixing matrix element.

We have applied our formalism to the reaction $J/\Psi \to \phi\pi^0\eta$ and give what we consider the best and most comprehensive prediction to date for this decay channel. The corresponding measurement will soon be possible with the upgraded BESIII detector [38].

In addition we addressed the following items:

(1) As it is illustrated in Fig. 6, although the kaon loop effect dominates the isospin-violating signal, the presence of isospin-violating coupling constants introduces a significant additional enhancement by roughly 50% (corresponding to a 20% effect on the amplitude level). To the order we are working, isospin violation in the vertices and in the kaon masses are of the same origin (i.e. are calculated from the same chiral Lagrangian), and no additional parameters enter.

(2) The effect of soft photon exchange in the meson propagation is small, even in the signal region, and amounts to a reduction of the signal by 10% (or 5% on the amplitude level).

(3) Neither of the two additional effects studied in this work, associated with an isospin-violating production operator, distorts the shape of the signal severely, cf. gray band vs solid line in Fig. 7.

(4) We have confirmed that the isospin violation in the final-state interaction, which can be identified with a_0–f_0 mixing, is much more important than isospin violation in the production operator. We therefore confirm the corresponding claim of Refs. [20,21] for the particular case of the reaction $J/\Psi \to \phi\pi^0\eta$.

Our final results are presented for a particular reaction. However, the formalism to calculate the propagating a_0–f_0 system in the presence of isospin violation is very general and therefore could also be used for the analysis of other experiments, once data is available. Especially items 1–3 of the list given above are independent of the reaction studied, and ought to be distinctly different from predictions of models viewing a_0 and f_0 as $q\bar{q}$ or four-quark systems, which allow for direct mixing without two-kaon-threshold enhancement. We hence conclude that it is indeed possible to measure and interpret a_0–f_0 mixing.

ACKNOWLEDGMENTS

We wish to thank Timo Lähde for very helpful communications and Email exchanges, and, in particular, for making preliminary fit results and numbers on the three-channel generalization of Ref. [24] available to us. B. K. and J. R. P. are grateful for the hospitality of the Institut für Kernphysik at the Forschungszentrum Jülich in the initial stage, and B. K. for that of the Facultad de Ciencias Físicas at the Universidad Complutense Madrid in the final stage of this project. The authors acknowledge partial financial support by the EU I3HP Project (RII3-CT-2004-506078). B. K. was supported by the DFG (SFB/TR 16). The research of J. R. P. was partially funded by Spanish CICYT Contracts No. FPA2005-02327 and No. FIS2006-03438, as well as Banco Santander/Complutense Contract No. PR27/05-13955-BSCH.

APPENDIX A: CHARGE VS ISOSPIN BASIS

The two-meson states of definite isospin (in the S-wave) are related to the states in the charge basis by the following relations:

$$\begin{pmatrix} |\pi\pi\rangle_{I=2} \\ |\pi\pi\rangle_{I=0} \\ |\eta\eta\rangle_{I=0} \\ |K\bar{K}\rangle_{I=0} \\ |K\bar{K}\rangle_{I=1} \\ |\pi^0\eta\rangle_{I=1} \end{pmatrix}_{J=0} \equiv \begin{pmatrix} -\sqrt{1/6} & \sqrt{1/3} & 0 & 0 & 0 & 0 \\ -\sqrt{1/3} & -\sqrt{1/6} & 0 & 0 & 0 & 0 \\ 0 & 0 & 1/\sqrt{2} & 0 & 0 & 0 \\ 0 & 0 & 0 & -\sqrt{1/2} & -\sqrt{1/2} & 0 \\ 0 & 0 & 0 & -\sqrt{1/2} & \sqrt{1/2} & 0 \\ 0 & 0 & 0 & 0 & 0 & 1 \end{pmatrix} \begin{pmatrix} |\pi^+\pi^-\rangle \\ |\pi^0\pi^0\rangle \\ |\eta\eta\rangle \\ |K^+K^-\rangle \\ |K^0\bar{K}^0\rangle \\ |\pi^0\eta\rangle \end{pmatrix}_{J=0}, \tag{A1}$$

where $|\pi^+\pi^-\rangle$ denotes the symmetrized combination of $|\pi^+\pi^-\rangle$ and $|\pi^-\pi^+\rangle$. The additional factors of $1/\sqrt{2}$ for the $\pi\pi$ and the $\eta\eta$ states account for Bose symmetry. Using the isospin basis for our calculation is particularly convenient as we consider production of states with definite isospin ($I = 0$ mostly), and the final state $\pi^0\eta$ has definite isospin $I = 1$, too.

APPENDIX B: THE LOOP FUNCTION G

For two mesons A, B with masses M_A and M_B propagating in the loop, the elementary two-point function is given by

$$G_{AB}(s) = -\frac{1}{16\pi^2}\left\{\frac{\Delta}{s}\left[\log\frac{1+\Omega_A}{1+\Omega_B} - \log\frac{M_A}{M_B}\right] + \frac{\nu}{2s}\log\frac{(\nu\Omega_A + s - \Delta)(\nu\Omega_B + s + \Delta)}{(\nu\Omega_A - s + \Delta)(\nu\Omega_B - s - \Delta)} - \log\left[\frac{q_{\max}^2}{M_A M_B}(1+\Omega_A)(1+\Omega_B)\right]\right\}, \tag{B1}$$

where $\Delta = M_B^2 - M_A^2$, $\nu^2 = s^2 - 2s(M_A^2 + M_B^2) + \Delta^2$, $\Omega_{A,B} = \sqrt{1 + M_{A,B}^2/q_{\max}^2}$, and $q_{\max}$ is the cutoff. The form in Eq. (B1) is correct and unambiguous below the pseudothreshold, $s \le (M_A - M_B)^2$, and has to be continued analytically into other kinematical regions. As described in the text, the determination of $G_i(s)$ has to be chosen so that on the physical, right-hand, cut of the ith state, $\mathrm{Im}G_i(s) = \sigma_i(s)/16\pi = k_i/(8\pi\sqrt{s})$, where k_i stands for the corresponding center-of-mass momentum. In the equal-mass limit $M_A = M_B = M$, Eq. (B1) reduces to $G_{A=B}(s) = G(s)$,

$$G(s) = -\frac{1}{16\pi^2}\left\{\sigma\log\frac{\sigma\Omega + 1}{\sigma\Omega - 1} - 2\log\left[\frac{q_{\max}}{M}(1+\Omega)\right]\right\}, \tag{B2}$$

where $\sigma = \sqrt{1 - 4M^2/s}$, $\Omega = \sqrt{1 + M^2/q_{\max}^2}$.

APPENDIX C: POLYNOMIAL REMAINDERS OF THE SCALAR FORM FACTORS

The polynomial remainders of the scalar form factors as defined in Eq. (12), up to $\mathcal{O}(p^4)$ in ChPT, are given as

$$\begin{aligned}
R_\pi^n(s) &= \sqrt{\frac{3}{2}}\left\{1 + \mu_{\pi(\pi)} - \frac{\mu_{\eta(\pi)}}{3} + \frac{16M_\pi^2}{F_\pi^2}(2L_8^r - L_5^r) + \frac{8(2M_K^2 + 3M_\pi^2)}{F_\pi^2}(2L_6^r - L_4^r) + \frac{4s}{F_\pi^2}(2L_4^r + L_5^r)\right\},\\
R_\pi^s(s) &= \frac{\sqrt{3}}{2}\left\{\frac{16M_\pi^2}{F_\pi^2}(2L_6^r - L_4^r) + \frac{8s}{F_\pi^2}L_4^r\right\},\\
R_K^n(s) &= \frac{1}{\sqrt{2}}\left\{1 + \frac{2}{3}\mu_{\eta(K)} + \frac{16M_K^2}{F_K^2}(2L_8^r - L_5^r) + \frac{8(6M_K^2 + M_\pi^2)}{F_K^2}(2L_6^r - L_4^r) + \frac{4s}{F_K^2}(4L_4^r + L_5^r)\right\},\\
R_K^s(s) &= 1 + \frac{2}{3}\mu_{\eta(K)} + \frac{16M_K^2}{F_K^2}(2L_8^r - L_5^r) + \frac{8(4M_K^2 + M_\pi^2)}{F_K^2}(2L_6^r - L_4^r) + \frac{4s}{F_K^2}(2L_4^r + L_5^r),\\
R_\eta^n(s) &= -\frac{1}{3\sqrt{2}}\left\{1 - 3\mu_{\pi(\eta)} + 4\mu_{K(\eta)} - \frac{\mu_{\eta(\eta)}}{3} + \frac{16M_\eta^2}{F_\eta^2}(2L_8^r - L_5^r) + \frac{8(10M_K^2 - M_\pi^2)}{F_\eta^2}(2L_6^r - L_4^r)\right.\\
&\quad \left. - \frac{128(M_K^2 - M_\pi^2)}{3F_\eta^2}(3L_7 + L_8^r) + \frac{4s}{F_\eta^2}(6L_4^r + L_5^r)\right\},\\
R_\eta^s(s) &= -\frac{2}{3}\left\{1 + 2\mu_{K(\eta)} - \frac{4}{3}\mu_{\eta(\eta)} + \frac{16M_\eta^2}{F_\eta^2}(2L_8^r - L_5^r) + \frac{4(8M_K^2 + M_\pi^2)}{F_\eta^2}(2L_6^r - L_4^r)\right.\\
&\quad \left. - \frac{64(M_K^2 - M_\pi^2)}{3F_\eta^2}(3L_7 + L_8^r) + \frac{2s}{F_\eta^2}(3L_4^r + 2L_5^r)\right\},
\end{aligned} \tag{C1}$$

where $\mu_{i(j)}$ are the tadpole loop functions defined as

$$\mu_{i(j)} = \frac{M_i^2}{32\pi^2 F_i F_j}\log\frac{M_i^2}{\mu^2}, \tag{C2}$$

and this particular choice of decay constants $F_{i/j}$ is in accordance with Ref. [60]. The L_i^r are the standard low-energy constants defined in Ref. [61].

APPENDIX D: SCATTERING AMPLITUDES WITH ISOSPIN VIOLATION

In this Appendix we give a complete list of S-wave projected four-meson amplitudes derived from Eq. (18) for those channels that are charge- and strangeness-neutral, i.e. reactions linking the channels (1) $\pi^+\pi^-$, (2) $\pi^0\pi^0$, (3) $\eta\eta$, (4) K^+K^-, (5) $K^0\bar{K}^0$, and (6) $\pi^0\eta$ including isospin violation; see also Ref. [45]. Our normalization for the S-wave projection is given by

$$T_{ab}^{J=0}(s) = \frac{1}{2}\int_{-1}^{1} dz T_{ab}(s, t(s,z), u(s,z)). \tag{D1}$$

a, b refer to the numbering of the possible in- and out-channels 1–6 as given above; of course one has $T_{ab} = T_{ba}$. In the following list, for reasons of brevity we suppress the $J = 0$ superscripts:

$$\begin{aligned}
&T_{11} = 2T_{14} = T_{44} = \frac{s + 4\Delta_\pi}{2F^2}, \qquad T_{12} = \frac{s - M_{\pi^0}^2}{F^2}, \qquad T_{13} = \frac{1}{3}T_{22} = T_{23} = T_{66} = \frac{M_{\pi^0}^2}{3F^2},\\
&T_{15} = T_{45} = \frac{1}{2}T_{55} = \frac{s}{4F^2}, \qquad T_{16} = \frac{\epsilon}{3F^2}(4M_\pi^2 - 3s), \qquad T_{24} = T_{25} = \frac{s}{4F^2}(1 \pm 2\sqrt{3}\epsilon) \mp \frac{2\epsilon}{\sqrt{3}F^2}M_K^2,\\
&T_{26} = -T_{36} = -\frac{4\epsilon}{3F^2}(M_K^2 - M_\pi^2), \qquad T_{33} = \frac{4M_\eta^2 - M_{\pi^0}^2}{3F^2},\\
&T_{34} = \frac{3s}{4F^2}\left(1 - \frac{2\epsilon}{\sqrt{3}}\right) - \frac{2}{3F^2}(M_{K^+}^2 - \Delta_\pi)(1 - \sqrt{3}\epsilon), \qquad T_{35} = \frac{3s}{4F^2}\left(1 + \frac{2\epsilon}{\sqrt{3}}\right) - \frac{2M_{K^0}^2}{3F^2}(1 + \sqrt{3}\epsilon),\\
&T_{46} = \frac{1}{4\sqrt{3}F^2}\left(1 + \frac{2\epsilon}{\sqrt{3}}\right)(3s - 4(M_{K^+}^2 - \Delta_\pi)), \qquad T_{56} = -\frac{1}{4\sqrt{3}F^2}\left(1 - \frac{2\epsilon}{\sqrt{3}}\right)(3s - 4M_{K^0}^2).
\end{aligned} \tag{D2}$$

All amplitudes are normalized by a factor of $1/F^2$ which, at this accuracy, can arbitrarily be identified with any meson decay constant. For numerical evaluations, we use the convention that the overall $1/F^2$ factor is replaced by one $1/\sqrt{F_\phi}$ factor for every external meson ϕ in the process concerned; for a discussion on how and why this choice yields the best description of data, see Refs. [28,62].

APPENDIX E: NUMERICAL INPUT

In our calculations we use the masses $M_{\pi^+} = 139.57$ MeV, $M_{\pi^0} = 134.98$ MeV, $M_{K^+} = 493.68$ MeV, $M_{K^0} = 497.67$ MeV, $M_\eta = 547.8$ MeV, $M_{J/\Psi} = 3097$ MeV, and $M_\phi = 1020$ MeV. In addition, we need the decay constants $F_\pi = 92.4$ MeV, $F_K = 1.22F_\pi$, and $F_\eta = 1.3F_\pi$. The leading-order $\pi^0\eta$ mixing angle is $\epsilon = 0.01$. For the low-energy constants of order p^4 [61] needed for the polynomial terms of the scalar form factors, we use the numerical values $L_4^r = 0.84 \times 10^{-3}$, $L_5^r = 0.52 \times 10^{-3}$, $L_6^r = -0.18 \times 10^{-3}$, $L_7 = -0.40 \times 10^{-3}$, and $L_8^r = 0.15 \times 10^{-3}$ (all given at a scale $\mu = M_\rho$), as obtained in a three-channel generalization [60] of the formalism presented in Ref. [24]. From the same fit, we use the relative strength parameter of nonstrange to strange scalar source terms, $\lambda_\phi = 0.117$. In the loop function $G(s)$ (see Appendix B), we employ a cutoff $q_{\max} = 0.95$ GeV.

[1] C. R. Münz, J. Resag, B. C. Metsch, and H. R. Petry, Nucl. Phys. **A578**, 418 (1994).
[2] R. L. Jaffe, Phys. Rev. D **15**, 267 (1977).
[3] N. N. Achasov, Yad. Fiz. **67**, 1552 (2004) [Phys. At. Nucl. **67**, 1529 (2004)].
[4] J. Vijande, F. Fernández, A. Valcarce, and B. Silvestre-Brac, arXiv:hep-ph/0206263.
[5] R. L. Jaffe and F. E. Low, Phys. Rev. D **19**, 2105 (1979).
[6] J. R. Peláez, Phys. Rev. Lett. **92**, 102001 (2004).
[7] J. R. Peláez and G. Ríos, Phys. Rev. Lett. **97**, 242002 (2006).
[8] R. L. Jaffe, arXiv:hep-ph/0701038.
[9] J. D. Weinstein and N. Isgur, Phys. Rev. Lett. **48**, 659 (1982).
[10] J. D. Weinstein and N. Isgur, Phys. Rev. D **27**, 588 (1983).
[11] J. D. Weinstein and N. Isgur, Phys. Rev. D **41**, 2236 (1990).
[12] G. Janssen, B. C. Pearce, K. Holinde, and J. Speth, Phys. Rev. D **52**, 2690 (1995).
[13] E. van Beveren and G. Rupp, Eur. Phys. J. C **22**, 493 (2001).
[14] J. A. Oller and E. Oset, Nucl. Phys. **A620**, 438 (1997); **A652**, 407(E) (1999).
[15] V. Baru, J. Haidenbauer, C. Hanhart, Y. Kalashnikova, and A. Kudryavtsev, Phys. Lett. B **586**, 53 (2004).
[16] Yu. S. Kalashnikova, A. E. Kudryavtsev, A. V. Nefediev, C. Hanhart, and J. Haidenbauer, Eur. Phys. J. A **24**, 437 (2005).
[17] C. Hanhart, Yu. S. Kalashnikova, A. E. Kudryavtsev, and A. V. Nefediev, Phys. Rev. D **75**, 074015 (2007).
[18] N. N. Achasov, S. A. Devyanin, and G. N. Shestakov, Phys. Lett. **88B**, 367 (1979).
[19] O. Krehl, R. Rapp, and J. Speth, Phys. Lett. B **390**, 23 (1997).
[20] C. Hanhart, AIP Conf. Proc. **688**, 61 (2003).
[21] C. Hanhart, Phys. Rep. **397**, 155 (2004).
[22] J. A. Oller, E. Oset, and J. R. Peláez, Phys. Rev. D **59**, 074001 (1999); **60**, 099906 (1999); **75**, 099903(E) (2007).

[23] U.-G. Meißner and J. A. Oller, Nucl. Phys. **A679**, 671 (2001).
[24] T. A. Lähde and U.-G. Meißner, Phys. Rev. D **74**, 034021 (2006).
[25] A. Dobado and J. R. Peláez, Phys. Rev. D **56**, 3057 (1997).
[26] A. Dobado and J. R. Peláez, Phys. Rev. D **47**, 4883 (1993).
[27] A. Gómez Nicola and J. R. Peláez, Phys. Rev. D **65**, 054009 (2002).
[28] J. R. Peláez, Mod. Phys. Lett. A **19**, 2879 (2004).
[29] A. Dobado, M. J. Herrero, J. R. Peláez, and E. Ruiz Morales, Phys. Rev. D **62**, 055011 (2000).
[30] B. Kerbikov and F. Tabakin, Phys. Rev. C **62**, 064601 (2000).
[31] N. N. Achasov and G. N. Shestakov, Phys. Rev. Lett. **92**, 182001 (2004).
[32] N. N. Achasov and G. N. Shestakov, Phys. Rev. D **70**, 074015 (2004).
[33] A. E. Kudryavtsev and V. E. Tarasov, Pis'ma Zh. Eksp. Teor. Fiz. **72**, 589 (2000) [JETP Lett. **72**, 410 (2000)].
[34] A. E. Kudryavtsev, V. E. Tarasov, J. Haidenbauer, C. Hanhart, and J. Speth, Yad. Fiz. **66**, 1994 (2003) [Phys. At. Nucl. **66**, 1946 (2003)].
[35] A. E. Kudryavtsev, V. E. Tarasov, J. Haidenbauer, C. Hanhart, and J. Speth, Phys. Rev. C **66**, 015207 (2002).
[36] V. Y. Grishina, L. A. Kondratyuk, M. Büscher, W. Cassing, and H. Ströher, Phys. Lett. B **521**, 217 (2001).
[37] F. E. Close and A. Kirk, Phys. Lett. B **489**, 24 (2000).
[38] J. J. Wu, Q. Zhao, and B. S. Zou, Phys. Rev. D **75**, 114012 (2007).
[39] M. Ablikim *et al.* (BES Collaboration), Phys. Lett. B **607**, 243 (2005).
[40] H. Leutwyler, Int. J. Mod. Phys. A **22**, 257 (2007).
[41] T. N. Truong, Phys. Rev. Lett. **61**, 2526 (1988).
[42] A. Dobado, M. J. Herrero, and T. N. Truong, Phys. Lett. B **235**, 134 (1990).
[43] T. N. Truong, Phys. Rev. Lett. **67**, 2260 (1991).
[44] J. Gasser and H. Leutwyler, Nucl. Phys. **B250**, 517 (1985).
[45] N. Beisert and B. Borasoy, Nucl. Phys. **A716**, 186 (2003).
[46] B. Borasoy and R. Nißler, Eur. Phys. J. A **26**, 383 (2005).
[47] R. Urech, Nucl. Phys. **B433**, 234 (1995).
[48] M. Knecht and R. Urech, Nucl. Phys. **B519**, 329 (1998).
[49] B. Kubis and U.-G. Meißner, Nucl. Phys. **A699**, 709 (2002).
[50] A. Nehme and P. Talavera, Phys. Rev. D **65**, 054023 (2002).
[51] A. Nehme, Eur. Phys. J. C **23**, 707 (2002).
[52] B. Kubis and U.-G. Meißner, Phys. Lett. B **529**, 69 (2002).
[53] H. Osborn and D. J. Wallace, Nucl. Phys. **B20**, 23 (1970).
[54] J. Gasser and H. Leutwyler, Nucl. Phys. **B250**, 539 (1985).
[55] D. J. Broadhurst, J. Fleischer, and O. V. Tarasov, Z. Phys. C **60**, 287 (1993).
[56] M. Beneke and V. A. Smirnov, Nucl. Phys. **B522**, 321 (1998).
[57] J. Gasser, V. E. Lyubovitskij, A. Rusetsky, and A. Gall, Phys. Rev. D **64**, 016008 (2001).
[58] S. V. Bashinsky and B. Kerbikov, Yad. Fiz. **59N11**, 2054 (1996) [Phys. At. Nucl. **59**, 1979 (1996)].
[59] A. Kucukarslan and U.-G. Meißner, Mod. Phys. Lett. A **21**, 1423 (2006).
[60] T. A. Lähde (private communication).
[61] J. Gasser and H. Leutwyler, Nucl. Phys. **B250**, 465 (1985).
[62] S. Descotes-Genon, N. H. Fuchs, L. Girlanda, and J. Stern, Eur. Phys. J. C **34**, 201 (2004).